



Integrated Analysis of the Eocene Sakesar Formation: Depositional Environment, Microfacies, Geochemistry, and Reservoir Characteristics in the Potwar Basin, Pakistan

Syed Bilawal Ali Shah^{1*}, Khaira Ismail², Wan Zairani Wan Bakar³

1. Department of Geology, University of Malaya, Kuala Lumpur 50603, Malaysia.

2. Faculty of Science and Marine Environment, Universiti Malaysia Terengganu, Kuala Nerus 21030, Terengganu, Malaysia.

3. Oil and Gas Engineering, School of Chemical Engineering, College of Engineering, Universiti Teknologi Mara, 40450 Shah Alam, Selangor, Malaysia.

* Corresponding author: bilawalshah22@siswa.um.edu.my k.ismail@umt.edu.my zairani@uitm.edu.my

ABSTRACT

The current study aimed to evaluate the petroleum generation potential of the Sakesar Formation. This study interprets and presents a depositional environment model, microfacies, and geochemical and petrophysical data of the Eocene Sakesar Formation in the Potwar Basin, Pakistan. Twenty well-cutting samples from two wells and six fresh outcrop samples were thoroughly studied. Results of total organic carbon and Rock-Eval pyrolysis of Sakesar Formation sediments show fair to good TOC contents ranging from 1.2-1.67 wt%. S₂ values of samples showed fair to good generation potential. Sediments appear mature, having primarily mixed Type II-III kerogen with good oil/gas-generation potential. Three microfacies have been identified in the Sakesar Formation at the Tatral section: Bioclastic wacke-packstone, Lockhartia-rich mud-wackestone, and benthic foraminiferal wackestone. The microfacies of the Sakesar Limestone depict the deposition of the Sakesar Limestone from the distal middle ramp to restricted inner ramp settings. Petrophysical well logs analysis of the Sakesar Formation showed an average porosity of ~9.12%; the lithology was identified as limestone, having an average water saturation of ~22.32% and an average hydrocarbon saturation of ~77.68%. Thus indicating average to good reservoir properties with very good hydrocarbon saturation. Sakesar Formation sediments characteristics interpretation showed that it can act as both source rock and reservoir rock in the Potwar Basin.

Keywords: Sakesar Formation; Potwar Basin; Depositional environment; microfacies.

Análisis integrado de la Formación Sakesar del Eoceno: Ambiente deposicional, microfacies, geoquímica y características reservorio de la cuenca de Potwar, Pakistán

RESUMEN

El presente estudio busca evaluar el potencial de generación petrolífera de la formación Sakesar. Con ese fin este trabajo presenta e interpreta un modelo ambiental deposicional, con información de microfacies, geoquímica y petrofísica. Un total de veinte muestras cortadas y pulidas de dos pozos y seis afloramientos se estudiaron cuidadosamente. Los resultados de los análisis de carbono orgánico total y de pirólisis (Rock eval) de los sedimentos de la formación Sakesar muestran que los contenidos de carbono orgánico total son de regulares a buenos y oscilan entre 1.2 y 1.67 wt%. Los valores S₂ de las muestras tienen un potencial de generación entre regular y bueno. Los sedimentos se muestran maduros y tienen una mezcla primaria de kerógenos tipo II-III con un buen potencial de generación de petróleo y gas. Tres microfacies se han identificado en la sección Teatral de la formación Sakesar: wacke-packstone bioclástica, wackestone de barro rico en lockhartia y wackestone de foraminíferos bentónicos. Las microfacies de las calizas de Sakesar muestran que sus deposiciones desde la rampa media distal hasta configuraciones de rampa interior restringidas. Los análisis petrofísicos de registro de pozo de la formación Sakesar muestran una porosidad promedio de ~9.12%; la litología se identificó como caliza, con un promedio de saturación de agua de ~22.32% y un promedio de saturación de hidrocarburos de ~77.68%. Por ende, los resultados indican que en promedio las propiedades del reservorio son buenas con muy buena saturación de hidrocarburos. La interpretación de las características de los sedimentos de la formación Sakesar muestran que esta puede actuar como roca fuente o como roca reservorio en la cuenca Potwar.

Palabras clave: Formación Sakesar; Cuenca Potwar; ambiente deposicional; microfacies

Record

Manuscript received: 12/03/2023

Accepted for publication: 27/03/2023

How to cite this article:

Shah, S. B. A., Ismail, K., & Bakar, W. Z. W. (2024). Integrated Analysis of the Eocene Sakesar Formation: Depositional Environment, Microfacies, Geochemistry, and Reservoir Characteristics in the Potwar Basin, Pakistan. *Earth Sciences Research Journal*, 28(1), 17-27. <https://doi.org/10.15446/esrj.v28n1.107766>

1. Introduction

One of Pakistan's productive oil and gas basins is the Potwar Basin in the Upper Indus Basin. Since the Attock Oil Company's first commercial hydrocarbon discovery at Khaur in 1914, the basin has been the focus of hydrocarbon exploration for more than a century (Asif et al., 2011; Du and Wang, 2013; Shah, 2022). This basin covers two-thirds of eastern Pakistan. Numerous scholars have provided details on hydrocarbon source rock (Kadri, 1995; Imtiaz et al., 2017; Liu et al., 2023; Shah and Abdullah, 2017). Hydrocarbon traps in the Potwar Basin are structurally controlled and also include stratigraphic traps (Ren et al., 2022; Shah, 2022; Xu et al., 2022a; Yasin et al., 2021; Yu et al., 2021).

The Potwar Basin's primary hydrocarbon reservoir and source rocks are the Early-Eocene and Paleocene sedimentary rocks (Kadri, 1995; Xi et al., 2023; Yang et al., 2024; Zhu et al., 2022). Major oil and gas discoveries in the Potwar Basin are from the Sakesar and Chorgali formations (He et al., 2021; Shah, 2009; Shah, 2023; Yin et al., 2023a; Yin et al., 2023b). The average thickness of the Sakesar and Chorgali formations in the area is (141.43-182.88m). A study by Fazeelat et al. (2010) has found that shallow marine sediments in the Potwar Basin are organic-rich, prompting the need to evaluate the Sakesar's Formations depositional environment, source, and reservoir rock characteristics in the Potwar Basin at Tatral and Balkassar oilfield.

The novel contribution of this research lies in its comprehensive approach: for the first time, well cutting samples, along with outcrop and well logs, have been thoroughly studied to assess source rock generation potential, thermal maturity, kerogen type identification, forms of kerogen assemblages, depositional environment, and petrophysical properties. This investigation aims to estimate the properties of reservoir rocks and their generation potential and will use Rider 1986 criteria to evaluate it (Table 1). Moreover, this research employs three different methods to assess and evaluate the two most critical properties of the petroleum system, namely, source and reservoir rock properties. Previous researchers have studied different formations and they have used different techniques. For example, Ali et al. (2015) studied Sakesar Formation reservoir properties at Fimkassar oilfield, Asif and Tahira (2007) studied the Tobra and Khewra formation's geochemical properties at Fimkassar oilfield, Khan et al. (2017) have studied microfacies of the Chorgali Formation at Khair-E-Murat range. This study is both necessary and unique due to the scarcity of information regarding the comprehensive interpretation of source and reservoir rocks in the Balkassar oilfield, including an understanding of the potential of proven source and reservoir rocks. The study area Balkassar and Tatral Section is located in Potwar Basin (Fig. 1).

The output of this study will establish the depositional environment, source generation potential, type of kerogen, thermal maturity of source rocks, forms of kerogen present and presence of possible hydrocarbons and the reservoir rocks in the subsurface of Balkassar oilfield. This research will have direct applicability to future hydrocarbon exploration by oil and gas companies.

Table 1. Qualitative description of reservoirs porosity set by Rider's (1986).

Porosity Evaluation on a Qualitative Basis	
Qualitative description	Average Porosity
Negligible	0-5%
Poor	5-10%
Good	10-20%
Very Good	20-30%
Excellent	More than 30%

2. Geological setting

The Potwar Basin is situated on the western side of the Indian Shield which is a part of the Upper Indus Basin, is where the Tatral Section and Balkassar oilfield are located (Kadri, 1995; Khan et al., 2022; Wei et al., 2023; Xiao et al., 2023; Zhang et al., 2021). The fore-deep of the Indus Basin, which consists of depressions, a platform and an outer and inner folded zone, are its main features (Kadri, 1995; Kazmi and Jan, 1997; Liang et al., 2024). The Indus Basin is host to almost all of Pakistan's main hydrocarbons resources (Kadri, 1995; Ren et al., 2023; Yin et al., 2023c; Yang et al., 2023).

The Kalachitta-Margalla hill ranges borders the Potwar Basin to the north, the Salt Range to the south, the Jhelum River to the east, and the Indus River to the west (Jia et al., 2023; Shah and Abdullah, 2016; Yin et al., 2023d; Yu et al., 2022). The basin is characterised by tight, complicated folds extending east to west that are disturbed by steep angle faults and turned southward. The northernmost part of the basin is more extensively deformed (Aadil et al., 2014; Kazmi and Abbasi, 2002; Kazmi and Jan 1997; Riaz, 2022; Shah, 2009; Shah, 2022). In the western portion, there are a number of broad, moderate east-west folds, however, the eastern portion's strike abruptly shifts toward the northeast, and the structures are composed of massive synclines and anticlines (Shah, 2022; Tie et al., 2023; Jia & Zhou, 2023; Zhou et al., 2023).

2.1 A brief overview of the source and reservoir rocks of Potwar Basin

Most of the potential source rocks in the Potwar Basin are of Palaeocene and Eocene age, and the majority of the oil discoveries are within faulted anticline traps ranging from the Cambrian to the Miocene (Table 2). The Sakesar, Wargal, Lockhart, Hangu, and Patala formations are recognized as the key source rocks in the Potwar Basin (Dai et al., 2023; Hasany and Saleem, 2012; Shah, 2022). Reservoir rocks in the basin include Paleogene shelf carbonates, Miocene alluvial sandstones, Jurassic and Permian continental sandstones, along with Cambrian alluvial and shoreface sandstones (Aadil et al., 2014; Kazmi and Abbasi, 2002). Notable reservoir rocks that have produced oil and gas in the Potwar Basin include the Jurassic Dutta, Cambrian Khewra, Jutana, Kussak, Tobra, Wargal, Amb, Margalla Limestone, Chorgali, Bhadrar, and Murree formations (Fazeelat et al., 2010; Ihsan et al., 2022; Kazmi and Jan, 1997).

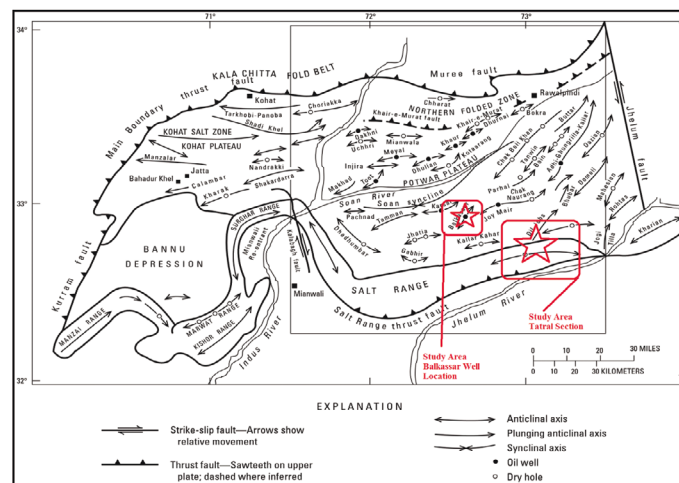
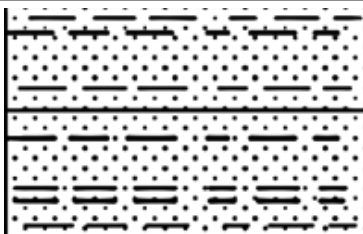
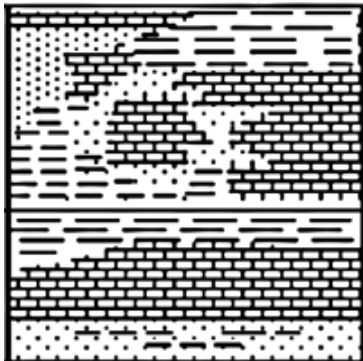
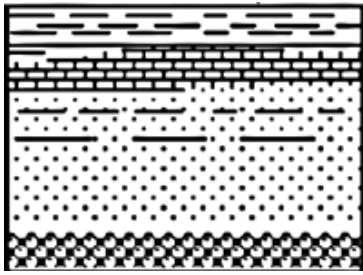
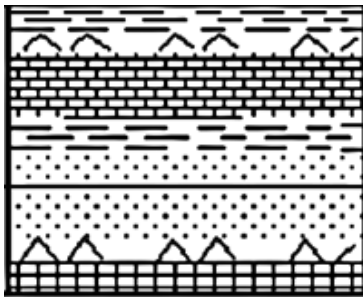


Figure 1. Tectonic Features of Potwar Basin

(Kadri, 1995; Shah, 2022; Zhou et al., 2023).

Table 2. Stratigraphy of the Potwar Basin in general (after Zahid et al., 2014; Shah, 2023).

AGE / EPOCH		LITHOLOGY	FORMATION	LITHOLOGY DESCRIPTION
Neogene	Pliocene		Nagri Chinji	Sandstone, sandstone and clay
	Miocene		Kamlial Murree	Sandstone, sandstone, limestone
	Oligocene			
Oligocene		Unconformity		
Paleogene	Eocene		Chorgali Sakesar	Limestone, limestone
	Paleocene		Patala Lockhart Hangu	Shale, limestone, sandstone
Mesozoic & Late Permian		Unconformity		
Jurassic			Datta	Sandstone, Shale
Permian	Early Permian		Chhidru Wargal Amb Sardhai Warcha Dandot Tobra	Sandstone, limestone, limestone, siltstone, interbeds of sandstone, shale interbeds of sandstone, sandstone and conglomerate.
Carboniferous to Ordovician		Unconformity		
Cambrian to Precambrian	Cambrian		Baghanwala Jutana Kussak Khewra	Shale, dolomite, sandstone and siltstone, Shale interbeds of dolomite and siltstone
	Infra-Cambrian		Salt Range	Marl, claystone and siltstone, Salt

3. Materials and Methods

A thorough geological field survey was carried at the type section of the Sakesar Formation (Tatral Section) was sampled at latitude 32°43'38.85"N, longitude 72°56'7.13"E for sampling (Fig. 2). Assaad (2008) and Tucker (2003) standard field procedures were used for sampling.

Eight outcrop samples were extracted after digging to minimise the effects of weathering. For microfacies analysis, six representative rock samples were used. As samples must be collected from unweathered material in outcrops. Therefore, a fresh section of the outcrop should be exposed to obtain representative samples, this would require a trench to be cut through

the exposed weathering zone using hand equipment, and sampling should be continuous and must evenly represent the entire interval being sampled. The exposed section to be sampled must be cleaned of all debris down to the lowest strata to be sampled. Once the exposed top layer was cleaned, a channel was excavated through the existing outcrop to expose fresh, unweathered material. This channel was extended down to the lowest strata to be sampled. Samples were then taken using a geological hammer, where harder, more resistant rock material was present. In order to support the analytical interpretation, field images of the diagnostic field characteristics were captured (Fig. 3). The Sakesar Formation, which has the lower confirmable contact with Nammal

Formation in the study area, is made up of light to medium and dark grey to brown, cherty, fractured, and occasionally nodular limestone, the formation was approximately 70 m thick. The Scanning Electron Microscope (SEM) was used for the micritic sediments and high-resolution photomicrographs to interpret microfacies present in the Sakesar Limestone.

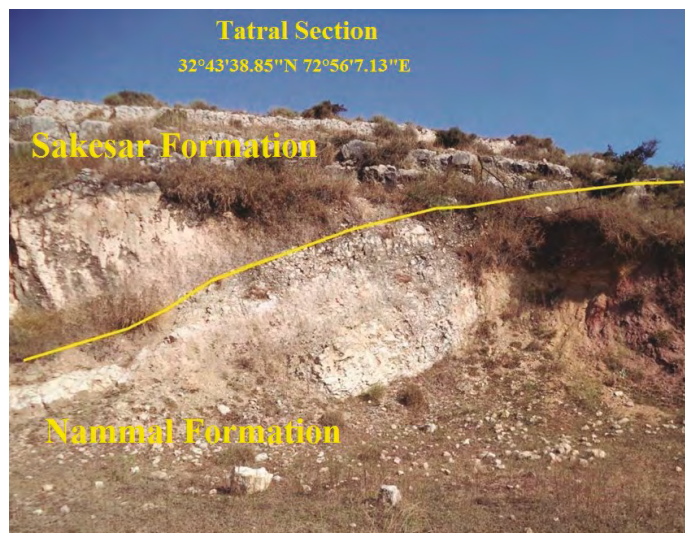


Figure 2. Showing the exposed section of Sakesar Formation in Tatral Section, also displaying its conformable contact with Nammal Formations.

Age	Formation	Sample	Thickness (m)	Lithology	Micrographs	Legends	Depositional Environment		
Eocene	Sakesar Limestone	3	25			Nodular limestone	Inner ramp	Mid ramp	Outer ramp
		2	30			Thin-Medium bedded limestone			
		1	15			Thick bedded limestone			

Figure 3. Litholog of the Sakesar Limestone at the study area.

Twenty well cutting samples were obtained from a well of the Balkassar oilfield in the Potwar Basin. The sediments were from Eocene sequence. The samples from well were obtained at intervals of 2–3 m interval. The details of the samples are provided in Table 3 and 4.

Reservoir rock characteristics were established using various logs: density, neutron, gamma ray, resistivity and spontaneous potential logs. Criteria from Rider (1986) and Shah and Shah (2021) were used to qualitatively describe the reservoir properties. This study used a set of well logs from Well A to investigate the Chorgali Formation's reservoir potential. Shah (2022), Shah and Shah (2021) and Hartmann and Beaumont's (1999) methods were used in this study to evaluate reservoir rock characteristics. Additionally, the hydrocarbon saturation, porosity, water saturation, and formation water resistivity were all calculated.

Table 3. Summary of analysed sediments of Sakesar Formations in Balkassar well 8.

Formation Name and No of samples	Depth (m)	Petroleum Potential				Maturity of sample Tmax °C	Quality of OM HI	Kerogen Type	Source rock generative potential
		TOC wt. %	S1	S2	S3				
Sakesar (20)	2447-2499	1.2-1.67	0.98-1.24	3.6-5.25	0.4-0.7	438-443	265-386	Mixed Type II/III	Fair to good

Table 4. Geochemical results of the sediments of Balkassar well 8.

Formation	Depth m	TOC %	Tmax °C	S1	S2	S3	PI	HI	OI	S2/S3	VR
Sakesar	2447	1.23	441	1.14	3.86	0.4	0.31	314	34.1	9.19	0.8
	2449	1.36	442	1.09	3.6	0.4	0.23	265	27.9	9.47	0.8
	2451	1.45	441	1.24	4.67	0.4	0.33	322	24.1	13.3	0.8
	2453	1.24	439	1.09	4.36	0.7	0.2	352	52.4	6.71	0.7
	2456	1.28	440	1.18	4.2	0.8	0.22	328	63.3	5.19	0.8
	2458	1.3	442	1.21	4.91	0.7	0.2	378	50	7.55	0.8
	2460	1.5	443	1.07	5.2	0.6	0.17	347	38	9.12	0.8
	2462	1.42	439	0.98	5.25	0.8	0.31	370	54.2	6.82	0.7
	2465	1.27	440	1.13	4.75	0.9	0.19	374	66.9	5.59	0.8
	2467	1.27	441	1.08	3.7	0.7	0.23	291	57.5	5.07	0.8
	2469	1.4	439	1.02	4.63	0.7	0.18	331	56.43	0.06	0.7
	2471	1.3	438	1.21	5.02	0.8	0.19	386	62.3	6.2	0.7
	2474	1.54	440	1.18	4.5	0.8	0.21	292	50.6	5.77	0.8
	2476	1.67	439	0.98	4.8	0.7	0.17	287	41.9	6.86	0.7
	2478	1.34	442	1.14	4.85	0.8	0.19	362	61.2	5.92	0.8
	2480	1.2	440	1.1	4.48	0.8	0.2	373	62.5	5.97	0.8
	2483	1.47	441	1.24	4.1	0.7	0.28	279	47.6	5.86	0.8
	2485	1.6	439	1.08	5.23	0.7	0.17	328	43.1	7.61	0.7
	2487	1.51	441	1.06	4.7	0.6	0.18	311	42.4	7.34	0.8
	2490	1.35	442	1.14	4.97	0.8	0.19	368	55.6	6.63	0.8

3.1 Organic Geochemical

Well fresh cutting samples were treated with acid to remove any carbonate minerals and weathered material prior to analysis. Samples were then crushed to less than 200 mesh, and TOC was then determined using LECO elemental analyzers CS-125. Additionally, pyrolysis was carried out using Rock-Eval VI. About 100mg of crushed samples were subjected to pyrolysis analysis in

a helium environment that was heated to 600°C. Pyrolysis generated the free hydrocarbons (S1), the amount of hydrocarbons produced by thermal cracking (S2), and Tmax, which are the three most crucial parameters (Baker, 1979; Espitalié et al., 1985; Peters, 1986). The hydrogen index and production yield were two other significant factors that were determined.

3.2 Well Log Analysis

The well logs in the LAS file format (.CSV file format) were used on the interactive petrophysics software package to determine reservoir properties to estimate various important reservoir characteristics.

The procedure for obtaining various parameters from the well logs is described in the section below:

The log track parameters that were directly read included:

1. Formation depth (ft)
2. Neutron porosity (NPHI; 0.45 to -0.15 scale)
3. Bulk resistivity of the formation (LLD; 0 – 2000ohm.m scale)
4. Spontaneous potential (SP; 0 – 100mv scale)
5. Bulk density of formation (RHOB; 1.95 – 2.95 scale)

Hydrocarbon Saturation (SH)

Spontaneous potential (SP) method (Figure 4, 5 and 6) was used for the determination of hydrocarbons at the zone of interest. The graphs and equations used together in the following process:

1. The wireline log report showed a bottom-hole temperature (BHT) of 180°F and a surface temperature (Ts) of 72°F, which were utilized in the equation (Fig. 4). The following equation was used to calculate the formation temperature (Tf):

$$T_f = T_s + D_f (\text{BHT} - T_s / \text{TD})$$

Where

Ts = Surface temperature

Tf = formation temperature

TD = Total depth

Df = Depth to the formation

2. Mud Filtrate Resistivity (Rmf) and Resistivity of Mud at Formation Temperature (Rmf) were corrected (Fig. 5).
3. Self-Potential (SP) was directly determined from the log chart SP curve.
4. The value of the Rmf/Rwe (equivalent water resistivity) ratio was measured (Fig. 6).
5. The equivalent water resistivity (Rwe) was calculated by dividing the corrected Rmf value by the Rmf/Rwe value ratio.
6. The equation for Rwe is as follows:

$$R_{we} = R_{mf} / (R_{mf} / R_{we})$$

Where

Rmf = equivalent mud filtrate resistivity

7. The equation in Figure 4 was used to convert Rwe to Rw, and the correct Rw value was determined using the Rwe value derived in step 5.
8. Archie's equation was used to estimate water saturation (Sw):

$$S_w = \sqrt{\frac{R_w}{\phi^m * R_t}}$$

9. The following equation can be used to estimate the saturation of a hydrocarbon (Sw) at a particular temperature :

$$S_H = 1 - S_w$$

After measuring the resistivity values of the mud filtrate, they were converted to equivalent mud filtrate resistivity values using the equation in Figure 4. To obtain the equivalent water resistivity, the equivalent mud filtrate resistivity values were used according to step 6. Subsequently, the equivalent water resistivity was converted to water resistivity, which was then used to determine water saturation using Archie's equation.

The log header's mud filtrate resistivity was determined at surface temperature. To determine the mud filtrate resistivity at formation temperature, it must be corrected to formation temperature for each value at a certain depth, and this correction was made using the equation presented in Figure 5.

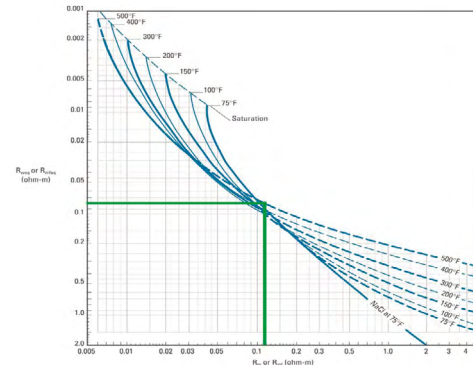


Figure 4. R_w is determined by determining R_{we} (Schlumberger, 1977).

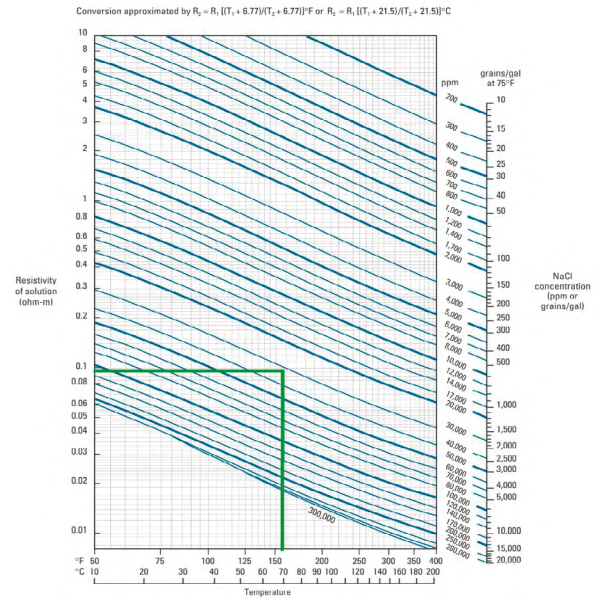


Figure 5. According to temperature R_{mf} and R_{we} correction (Schlumberger, 1977).

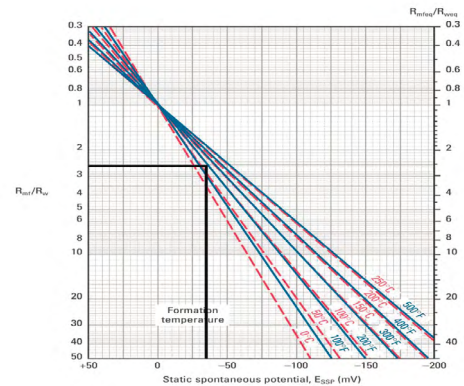


Figure 6. Determination of R_{mf}/R_{we} based on Self-Potential (Schlumberger, 1977).

4. Results and Discussion

4.1 Microfacies analysis and depositional environment

The Sakesar Formation is comprised of light-medium grey to dark light grey, massive, nodular limestone and petrographically, it mainly comprises of wackestone depositional texture (Shah, 2009; Shah, 2023; Shah et al., 2023).

Bioclastic wackestone (Plate 1)

Limestone that makes up this microfacies is light grey, nodular, fractured, and medium to thick bedded (Fig 7). The microfacies is characterized mainly by bioclasts, the orthochem of the microfacies is micrite matrix mainly. The orthochem micrite matrix exhibits a state of calm and low energy conditions.

Depositional Environment

The bioclasts of various echinoids and algae scattered in microscopic environments are the primary allochems of this microfacies. This microfacies is consistent with an inner ramp depositional environment based on the faunal composition and depositional texture of the wackestone.

Lockhartia rich Mud wackestone (Plate 2)

It is made up of thickly bedded, cherty, nodular, light to dark grey limestone. The Lockhartia-dominant allochems of larger benthic foraminifera, followed by the Assilina species of larger benthic foraminifera, with echinoids and bioclasts of certain larger benthic foraminifera, are mostly what distinguish the microfacies.

Depositional Environment

The dominant orthochem of this microfacies is a micrite matrix, while the primary allochems include Lockhartia species, Assilina sp., bioclasts of echinoids, and Rotalia, with larger benthic foraminifera being notable. Lockhartia is indicative of inner ramp settings, whereas Assilina is associated with mid-ramp environments, according to Ghose (1977), Racey (1994), and Shah (2009).

Benthic foraminiferal wackestone (Plate 3)

This microfacies is composed of medium- to thick-bedded, light to pale grey nodular, and highly fractured limestone. The larger benthic foraminifera, rovalia species, and several echinoids comprise the majority of the allochems that characterize the plate 2 microfacies. Additionally, bioclasts of several larger and smaller benthic foraminifera are included in the allochems of this microfacies.

Depositional Environment

The micritic covering on the skeletal grains, according to Flugel et al. (2010), suggests deposition in the photic zone at a depth of less than 100 to 200 m. The predominance of larger benthic foraminifera, which are dispersed in micritic matrix, demonstrates very calm and low-energy conditions (Fig. 8).

4.2 TOC and Rock-Eval Pyrolysis

Commonly, organic richness is represented by TOC wt% (Peters, 1986; Peters and Cassa, 1994). According to Baker, (1979) and Espitalié et al. (1977), for clastic rocks to be considered a source rock, it should have a minimum TOC value of 1.0%. The Sakesar Formation sediments TOC contents ranges from 1.2-1.67 wt%. These data indicates that the majority of the samples possessed fair to good potential as per TOC results however TOC itself is not an enough source to be relied on it only, as it is just a screening/initial method. Additionally, the samples with thermal maturity would have greater original TOC values than the TOC values at this time since TOC content declines with increasing thermal maturity (Li et al., 2023; Peters, 1986; Su et al., 2023; Wang et al., 2023; Xu et al., 2022b).

According to Peters and Cassa (1994), the S2 parameter, which is obtained during pyrolysis, is the most indicative measure for assessing the potential of hydrocarbons generation. According to Baker, (1979) and Espitalié et al. (1977), at least 5mg HC/g S2 is essential for good petroleum generation potential. Generally, the hydrocarbon (S2) yields ranged from 3.6-5.25 mg/g

in Sakesar Formation. S2 vs TOC cross plot (Fig. 9) indicated fair to good petroleum generation potential.

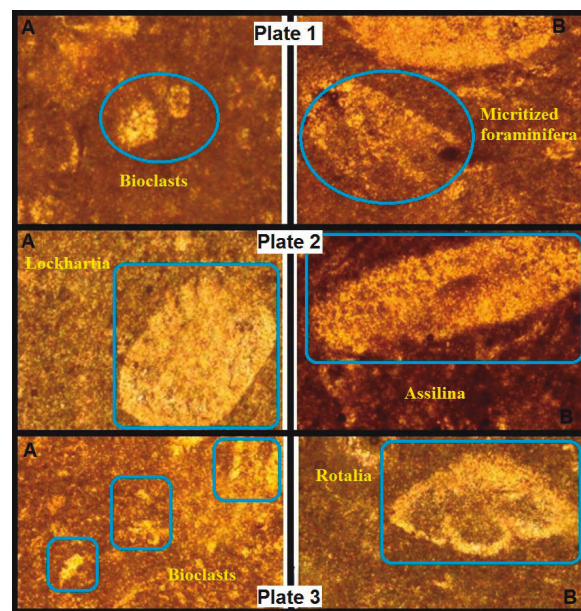


Figure 7. Plates: Microfacies of the Sakesar Formation in the studied area. Plate 1 (A) Bioclasts, (B) Micritized foraminifera, Plate 2 (A) Lockhartia, (B) Assilina, Plate 3 (A) Bioclasts, (B) Rotalia.

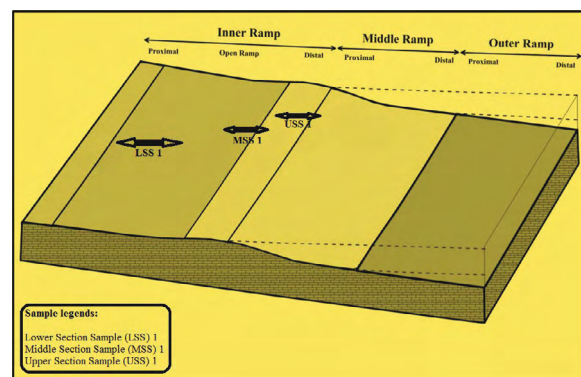


Figure 8. Depositional model of Sakesar Formation on the basis of samples analysed.

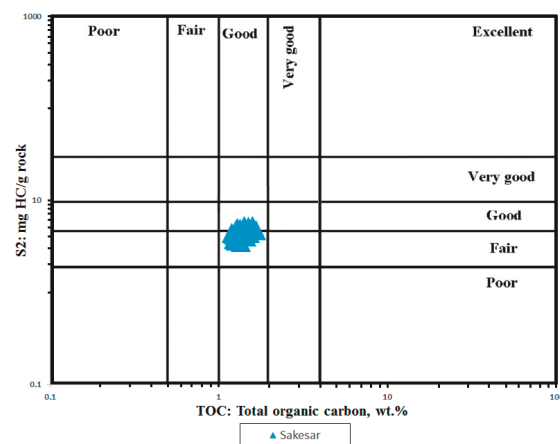


Figure 9. Plot comparing Pyrolysis S2 values and total organic carbon (TOC) to illustrate the potential of the analyzed samples as source rocks for generating hydrocarbons.

Using the migration index (S1/TOC), it is possible to differentiate between indigenous and migrated petroleum (Peters, 1986), the examined samples were indigenous, as indicated by the migration index, S1 vs TOC (Fig. 10).

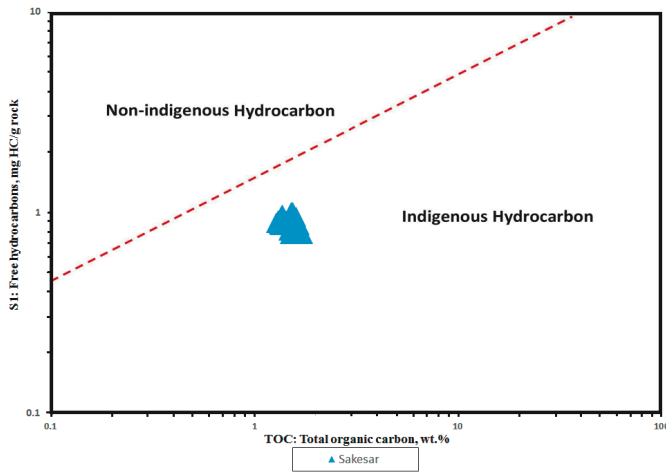


Figure 10. S1 vs TOC plot for migration index.

4.2 Kerogen Type

HI is the hydrogen index (mgHC/g TOC) which is used to characterize the origin of organic matter (Baker, 1979). HI values for the Sakesar Formation ranged between 265-386 mg HC/g TOC. For kerogen classification, samples pyrolysis data were used HI vs Tmax plot. All examined sediments mostly have mixed type-II/III kerogen. The type of kerogen identified by S2 vs TOC plots was also in agreement with the HI vs Tmax plot (Fig. 11).

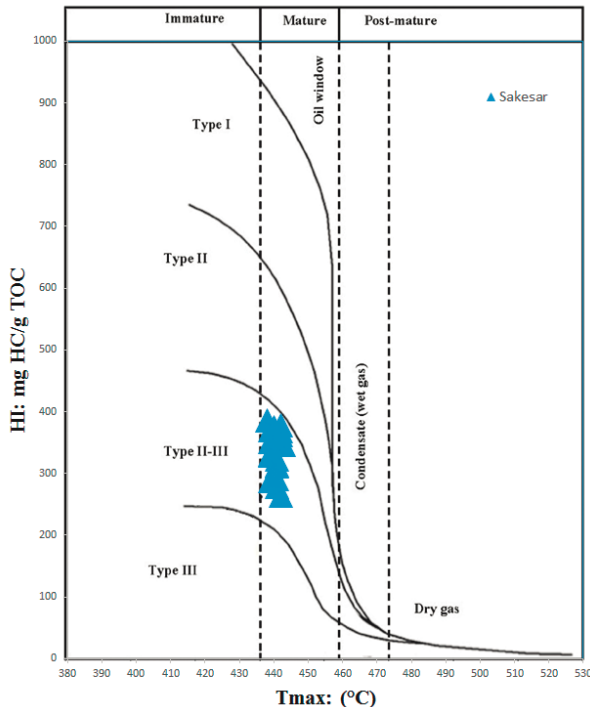


Figure 11. HI vs Tmax plot for kerogen type.

4.3 Thermal Maturity

In this study, three maturity indicators were utilized for thermal maturity including Tmax, vitrinite reflectance (%Ro), and the Production index. Vitrinite reflectance values ranging 0.6–1.3%Ro is mature, capable of generating oil (Brooks and Welte, 1984; Tissot, 1984; Waples, 1985). Tmax values varied widely, with values from 435 to 465 °C reflecting type III kerogen and values from 430 to 455 °C representing types I and II (Espitalié, 1977).

The observed vitrinite reflectance values for the Sakesar Formation ranged from 0.72 to 0.81%, with a Tmax of 438 to 443 °C, suggesting the peak of the oil generation window (Table 3) (Fig. 12).

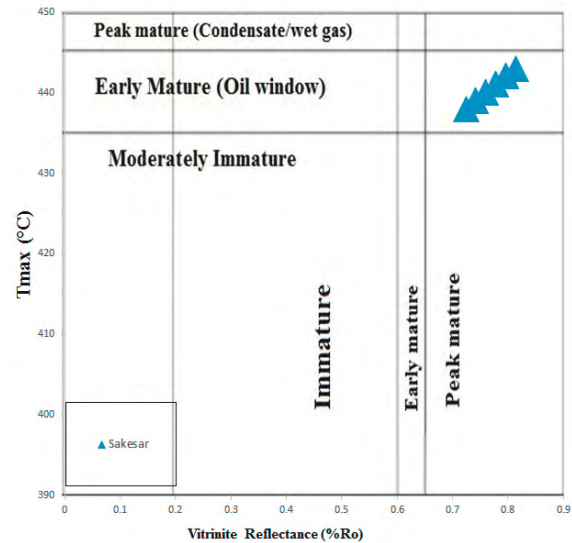


Figure 12. Plot of Tmax versus Vitrinite Reflectance (Ro) showing the maturity levels.

The Rock-Eval Tmax parameter is used to assess the maturity of kerogen in sedimentary rocks, which is crucial for hydrocarbon exploration, Tmax represents the temperature at which maximum hydrocarbon generation occurs from kerogen during pyrolysis, a laboratory simulation of natural thermal degradation, as kerogen matures under geological conditions, its ability to generate hydrocarbons increases, reflected in a higher Tmax value, therefore, a rising Tmax indicates more mature kerogen, helping geologists identify potential hydrocarbon source rocks and their evolutionary stage ranging from immature, through the optimal oil window, to overmature gas-producing stages (Baker, 1979; Welte, 1972; Waples, 1985). There are many factors that can influence the Tmax according to Espitalié et al. (1985) such as migrated hydrocarbons, a low pyrolysis response and oil-based mud. According to Mahdi et al. (2022) and Jarvie et al. (2001) samples have the highest Tmax values when the S2 > 0.50-mg/g rock. The analysed sediments had S2 > 1-mg/g rock (Table 3 and 4). The measured Tmax values of the samples ranged from 438 °C to 443 °C. According to Peters (1986) the results shows the presence of mature organic material.

The maturity of organic matter can be assessed by comparing the amount of hydrocarbons it has already generated (S1) with its total potential hydrocarbon yield. This comparison involves calculating the production index (PI), which is the sum of S1 and the remaining potential hydrocarbons (S2), as described by Collins (1975) and Romanchev (1979). For Type I and Type II kerogen PI value is more than 0.1, whereas the typical PI value range for Type III kerogen is between 0.1 and 0.2, the samples are considered immature if PI values are < 0.15, the samples are considered mature if the PI values ranges between 0.15-0.4 and the samples are considered over-mature if the values are > 0.4 (Peters, 1986; Bacon et al., 2000).

The PI values for the sediments from the Sakesar Formation in this study ranged from 0.17 to 0.33, thus indicating a maturity level reaching the oil window (Fig.13), which is in agreement with the Tmax and vitrinite reflectance data.

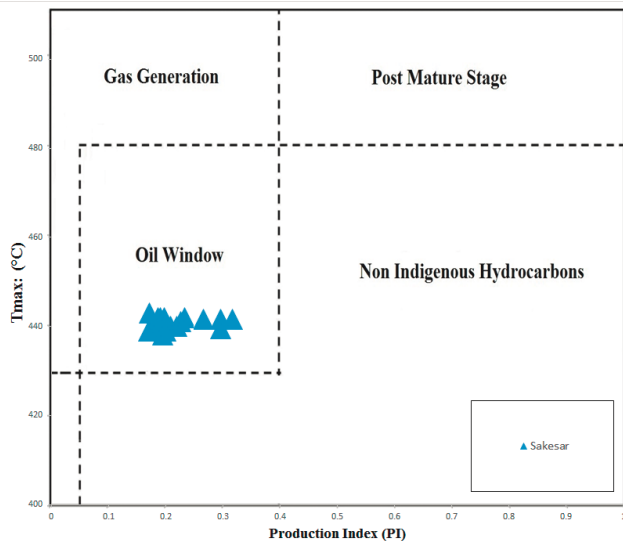


Figure 13. Tmax vs production index (PI) plot.

4.4 Reservoir potential

The reservoir parameters determined from the petrophysical analysis were used for quantitative interpretation of the reservoir. The estimated petrophysical characteristics of the Sakesar Formation are shown in Table 5. The average porosity was 9.12%, showing poor to moderate reservoir potential, whereas higher porosity is observed in the middle and top portion of the Formation (8028-8113ft) where as low porosity is observed at the higher depth of the formation. According to Rider's (1986) Shah and Shah (2021) criteria, the average water saturation was 22.32%, and the hydrocarbon saturation was 77.68%, indicating an average to good hydrocarbon potential (Table 1).

Table 5. Various well logs calculated parameters for different properties estimation.

Depth (ft)	Temp	RHOB	Φ_D	SP	Φ (N.D)	Rt (LLD)	Rwe	Rw	Sw	SH	Lithology
8028	153	2.69	0.4	-25	0.22	610	0.4	0.7	24%	76%	Limestone
8056	154	2.72	0.3	-16	0.19	1230	0.5	0.8	37%	63%	Limestone
8084	154	2.65	0.1	-29	0.17	1520	0.4	0.7	26%	74%	Limestone
8113	155	2.62	0.2	-36	0.19	1840	0.3	0.3	16%	84%	Limestone
8141	156	2.53	0.1	-44	0.13	1610	0.3	0.6	23%	77%	Limestone
8169	156	2.59	0.3	-35	0.14	166	0.3	0.4	14%	86%	Limestone
8198	157	2.46	0.2	-32	0.11	890	0.3	0.4	17%	83%	Limestone

5. Discussion

5.1 Organic richness and Rock-Eval pyrolysis

According to Bordenave (1993), sediments must contain a significant quantity of organic richness, typically exceeding 2% total organic carbon (TOC) by weight, for hydrocarbons to be produced when they attain thermal maturity. According to Peters and Cassa (1994), The Total Organic Carbon (TOC) is a fundamental geochemical marker that quantifies the weight percentage of organic materials present, as highlighted by Peters (1986) and Shah (2023). Analysis of the samples reveals that most exhibit fair to good TOC levels, with several displaying very good TOC contents.

To enhance our comprehension of the generative potential, it is essential to utilize Total Organic Carbon (TOC) data alongside other geochemical parameters, such as the S1 and S2 pyrolysis characteristics, as outlined by Peters and Cassa (1994) and Dembicki (2009). Consequently, to differentiate between non-indigenous and indigenous hydrocarbons, we employed both the S1 values and the TOC weight percentages. Analysis of the rock samples revealed that they consistently presented low S1 values and, conversely, high TOC levels, signifying the presence of native hydrocarbon sources. The majority of the examined sediments include mixed type-II/III kerogen. S2 vs TOC graphs and the HI vs Tmax plot both correctly identified the kind of kerogen (Fig. 11). As a result, the Sakesar Formation sediments have the potential to produce considerable amounts of hydrocarbons at the appropriate thermal maturities, as well as to contribute a significant amount to the oilfield's main petroleum system.

5.2 Microfacies analysis and depositional environment

Three microfacies have been identified based on the biogenic components, carbonate texture, and depositional fabric: Bioclastic wacke-packstone (Plate 1), Lockhartia rich Mud wackestone (Plate 2), and benthic foraminiferal wackestone (Plate 3). Assemblage of rotalia, echinoids, algae, and associated bioclasts, comprise the majority of the fauna in these microfacies. On the basis of these microfacies a depositional model has been constructed (Fig. 8).

5.3 Petrophysical analyses

Petrophysical analysis through wireline logs were conducted using spontaneous potential (SP) method. The upper and middle part of the Sakesar Formation from ~8028-8113 ft depth generally exhibits good porosity, the average porosity at most of the interpreted points is also in good potential range >10%. According to Amigun and Odole (2013) and Rider's (1986) criteria (Table 1), Sakesar Formation have good reservoir potential to produce hydrocarbons in Balkassar oilfield with moderate porosity and good hydrocarbon saturation.

6. Conclusions

The investigation of the Sakesar Formation sediments through microfacies analysis, geochemical analysis, and petrophysical analysis has yielded several key findings:

Microfacies Analysis: Three distinct microfacies were identified based on biogenic components, carbonate texture, and depositional fabric in the Sakesar Formation at the Tatal section: Bioclastic wacke-packstone, Lockhartia-rich Mud-wackestone, and benthic foraminiferal wackestone. The microfacies of the Sakesar Limestone suggest that it was deposited in restricted inner ramp settings extending to the distal middle ramp.

Geochemical Analysis: Source rock analyses, including S2, HI (Hydrogen Index), and Tmax values, indicate that the Sakesar formations possess fair to good potential for hydrocarbon generation. The presence of mixed type II/III kerogen is suggested by the S2 and HI values. Plots of S2 vs. TOC (Total Organic Carbon) and HI vs. Tmax position the sediments within the early maturity window, implying that the Sakesar Formation may have generated oil and gas.

Petrophysical Analysis: The Sakesar Formation exhibits average reservoir qualities but demonstrates good hydrocarbon saturation potential, indicating a promising capacity to produce hydrocarbons.

These findings collectively enhance our understanding of the Sakesar Formation's potential as a hydrocarbon source, underscoring the significance of integrated sedimentological, geochemical, and petrophysical analyses in evaluating petroleum systems.

Acknowledgments:

The Author is very thankful to University of Malaysia for providing lab facilities for this study.

References

- Aadil, N., & Sohail, G. M. (2014). 3D geological modelling of Punjab Platform, Middle Indus Basin Pakistan through Integration of wireline Logs and seismic data. *Journal of the Geological Society of India*, 83(2), 211–217. <https://doi.org/10.1007/s12594-014-0033-2>
- Ali, A., Kashif, M., Hussain, M., Siddique, J., Aslam, A., & Ahmed, Z. (2015). An Integrated Analysis of Petrophysics, Cross-Plots and Gassmann Fluid Substitution for Characterization of Fimkassar Area, Pakistan: A Case Study. *Arabian Journal for Science and Engineering*, 40, 181–193. <https://doi.org/10.1007/s13369-014-1500-1>
- Amigun, J. O., & Odole, O. A. (2013). Petrophysical properties evaluation for reservoir characterisation of Seyi oil field (Niger-Delta). *International Journal of innovation and applied studies*, 3(3), 756–773.
- Asif, M., & Tahira, F. (2007). Distribution and geochemical applications of aromatic hydrocarbons in crude oils. *Journal of Research (Science)*, 18, 79–90.
- Asif, M., Fazeelat, T., & Grice, K. (2011). Petroleum geochemistry of the Potwar Basin, Pakistan: 1. Oil–oil correlation using biomarkers, d13C and D. *Organic Geochemistry*, 42(10), 1226–1240. <https://doi.org/10.1016/j.orggeochem.2011.08.003>
- Assaad, F. A. (2008). *Field methods for petroleum geologists: A guide to computerized lithostratigraphic correlation charts case study*. Springer Science & Business Media, Northern Africa.
- Bacon, C. A., Calver, C. R., Boreham, C. J., Leaman, D. E., Morrison, K. C., Revill, A. T., & Volkman, J. K. (2000). The petroleum potential of onshore Tasmania: a review. *Geological Survey Bulletin*, 71, 1–93.
- Brooks, J., & Welte, D. H. (1984). *Advances in petroleum geochemistry*. U.S. Department of Energy Office of Scientific and Technical Information
- Collins, A. (1975). *Geochemistry of oilfield waters*. Elsevier.
- Dai, Z., Li, X., & Lan, B. (2023). Three-Dimensional Modeling of Tsunami Waves Triggered by Submarine Landslides Based on the Smoothed Particle Hydrodynamics Method. *Journal of Marine Science and Engineering*, 11(10), 2015. <https://doi.org/10.3390/jmse11102015>
- Dembicki Jr., H. (2009). Three common source rock evaluation errors made by geologists during prospect or play appraisals. *The American Association of Petroleum Geologists Bulletin*, 93(3), 341–356.
- Du, W., & Wang, G. (2013). Intra-Event Spatial Correlations for Cumulative Absolute Velocity, Arias Intensity, and Spectral Accelerations Based on Regional Site Conditions. *Bulletin of the Seismological Society of America*, 103(2A), 1117–1129. DOI: 10.1785/0120120185
- Espitalié, J., Deroo, G., & Marquis, F. (1985). La pyrolyse Rock-Eval et ses applications. Partie I. *Revue de l'Institut Français du Pétrole*, 40, 563–579. Partie II. 40, 755–784.
- Espitalié, J., Laporte, J. L., Madec, M., Marquis, F., Leplat, P., Paulet, J., & Boutefeu, A. (1977). Methode rapide de caracterisation des roches meres, de leur potentiel pétrolier et de leur degré d'évolution. *Revue de l'Institut Français du Pétrole*, 32(1), 23–42. <https://doi.org/10.2516/ogst:1977002>
- Fazeelat, T., Jalees, M. I., & Bianchi, T. S. (2010). Source rock potential of Eocene, Paleocene and Jurassic deposits in the subsurface of the Potwar Basin, northern Pakistan. *Journal of Petroleum Geology*, 33(1), 87–96. <https://doi.org/10.1111/j.1747-5457.2010.00465.x>
- Flügel, E. (2010). Microfacies and archaeology. In: E. Flügel (Ed.). *Microfacies of carbonate rocks*. Springer, Berlin, Heidelberg. https://doi.org/10.1007/978-3-642-03796-2_19
- Ghose, B. K. (1977). Paleocology of the Cenozoic reefal foraminifers and algae—a brief review. *Palaeogeography, Palaeoclimatology, Palaeoecology*, 22(3), 231–256. [https://doi.org/10.1016/0031-0182\(77\)90030-X](https://doi.org/10.1016/0031-0182(77)90030-X)
- Hartmann, D. J., & Beaumont, E. A. (1999). Predicting Reservoir System Quality and Performance. In: Beaumont, E. A. & Foster, N. H. (Eds.). *Treatise of Petroleum Geology/Handbook of Petroleum Geology: Exploring for Oil and Gas Traps*. American Association of Petroleum Geologists
- Hasany, S. T., & Saleem, U. (2012). An integrated subsurface geological and engineering study of Meyal field, Potwar plateau, Pakistan. *Search and Discovery Article*, 20151, 1–41.
- He, M., Dong, J., Jin, Z., Liu, C., Xiao, J., Zhang, F., & Deng, L. (2021). Pedogenic processes in loess-paleosol sediments: Clues from Li isotopes of leachate in Luochuan loess. *Geochimica et Cosmochimica Acta*, 299, 151–162. <https://doi.org/10.1016/j.gca.2021.02.021>
- Ihsan, S., Fazeelat, T., Imtiaz, F., & Nazir, A. (2022). Geochemical characteristics and hydrocarbon potential of Cretaceous Upper Shale Unit, Lower Indus Basin, Pakistan. *Petroleum Science and Technology*, 40(3), 257–269. <https://doi.org/10.1080/10916466.2021.1993913>
- Imtiaz, F., Fazeelat, T., Nazir, A., & Ihsan, S. (2017). Geochemical characterization of sediments samples of Sembar Formation from three different wells of Southern Indus Basin. *Petroleum Science and Technology*, 35(7), 633–640. <https://doi.org/10.1080/10916466.2016.1274757>
- Jarvie, D. M., Morelos, A., & Han, Z. (2001). Detection of pay zones and pay quality in the Gulf of Mexico: Application of geochemical techniques. *Gulf Coast Association of Geological Societies Transactions*, 51, 151–160.
- Jia, B., & Zhou, G. (2023). Estimation of global karst carbon sink from 1950s to 2050s using response surface methodology. *Geo-spatial Information Science*. <https://doi.org/10.1080/10095020.2023.2165974>
- Jia, S., Dai, Z., Zhou, Z., Ling, H., Yang, Z., Qi, L., & Soltanian, M. R. (2023). Upscaling dispersivity for conservative solute transport in naturally fractured media. *Water Research*, 235, 119844. <https://doi.org/10.1016/j.watres.2023.119844>
- Kadri, I. B. (1995). *Petroleum geology of Pakistan*. Karachi, Pakistan: Pakistan Petroleum Limited.
- Kazmi, A. H., & Jan, M. Q. (1997). *Geology and tectonics of Pakistan*. Karachi, Pakistan: Graphic publishers.
- Kazmi, A. H., & Abbasi, I. A. (2008). *Stratigraphy and historical geology of Pakistan*. Peshawar: Department & National Centre of Excellence in Geology press, 1st ed.
- Khan, M. Z., Rahman, Z. U., Khattak, Z., & Ishfaq, M. (2017). Microfacies and diagenetic analysis of Chorgali Carbonates, Chorgali Pass, Khair-E-Murat range: implications for hydrocarbon reservoir characterization. *Pakistan Journal of Geology*, 1(1), 18–23.
- Khan, N., Weltje, G. J., Jan, I. U., & Swennen, R. (2022). Depositional and diagenetic constraints on the quality of shale-gas reservoirs: A case study from the Late Palaeocene of the Potwar Basin (Pakistan, Eastern Tethys). *Geological Journal*, 57(7), 2770–2787. <https://doi.org/10.1002/gj.4439>
- Li, J., Zhang, Y., Lin, L., & Zhou, Y. (2023). Study on the shear mechanics of gas hydrate-bearing sand-well interface with different roughness and dissociation. *Bulletin of Engineering Geology and the Environment*, 82(11), 404. <https://doi.org/10.1007/s10064-023-03432-9>
- Liang, S., Zhao, Z., Li, C., Yin, Y., Li, H., & Zhou, J. (2024). Age and petrogenesis of ore-forming volcanic-subvolcanic rocks in the Yidonglinchang Au deposit, Lesser Xing'an Range: Implications for late Mesozoic Au mineralization in NE China. *Ore Geology Reviews*, 165, 105875. <https://doi.org/10.1016/j.oregeorev.2024.105875>

- Liu, W., Zhou, H., Zhang, S., & Zhao, C. (2023). Variable Parameter Creep Model Based on the Separation of Viscoelastic and Viscoplastic Deformations. *Rock Mechanics and Rock Engineering*, 56(6), 4629-4645. <https://doi.org/10.1007/s00603-023-03266-7>
- Mahdi, A. Q., Abdel-Fattah, M. I., & Hamdan, H. A. (2022). An integrated geochemical analysis, basin modeling, and palynofacies analysis for characterizing mixed organic-rich carbonate and shale rocks in Mesopotamian Basin, Iraq: Insights for multisource rocks evaluation. *Journal of Petroleum Science and Engineering*, 216, 110832. <https://doi.org/10.1016/j.petrol.2022.110832>
- Peters, K. E. (1986). Guidelines for evaluating petroleum source rock using programmed pyrolysis. AAPG Bulletin, 70, 318-329. <https://doi.org/10.1306/94885688-1704-11D7-8645000102C1865D>
- Peters, K. E., & Cassa, M. R. (1994). Applied source rock geochemistry. In: L.B. Magoon & W.G. Dow (Eds.). *The Petroleum System – From Source to Trap*. American Association of Petroleum Geologists Memoir 60. Tulsa, Oklahoma, USA, pp. 93–120.
- Racey, A. (1994). Biostratigraphy and palaeobiogeographic significance of Tertiary nummulitids (foraminifera) from northern Oman. *Micropalaeontology and Hydrocarbon Exploration in the Middle East*, 343, 370.
- Ren, C., Yu, J., Liu, X., Zhang, Z., & Cai, Y. (2022). Cyclic constitutive equations of rock with coupled damage induced by compaction and cracking. *International Journal of Mining Science and Technology*, 32(5), 1153-1165. <https://doi.org/10.1016/j.ijmst.2022.06.010>
- Ren, C., Yu, J., Zhang, C., Liu, X., Zhu, Y., & Yao, W. (2023). Micro-macro approach of anisotropic damage: A semi-analytical constitutive model of porous cracked rock. *Engineering Fracture Mechanics*, 290, 109483. <https://doi.org/10.1016/j.engfracmech.2023.109483>
- Riaz, M. (2022). Subsurface Structural Interpretation of Missa Keswal, Eastern Potwar, Pakistan. *Journal of Earth Sciences and Technology*, 3(2), 17-28.
- Rider, M. H. (1986). *The geological interpretation of well logs*. Blackie, Glasgow.
- Schlumberger. (1977). Log Interpretation Charts. Schlumberger Limited, New York.
- Shah, S. B. A., & Abdullah, W. H. (2016). Petrophysical properties and hydrocarbon potentiality of Balkassar well 7 in Balkassar oilfield, Potwar Plateau, Pakistan. *Bulletin of the Geological Society of Malaysia*, 62(1), 73-77.
- Shah, S. B. A., & Abdullah, W. H. (2017). Structural interpretation and hydrocarbon potential of Balkassar oil field, eastern Potwar, Pakistan, using seismic 2D data and petrophysical analysis. *Journal of the Geological Society of India*, 90(3), 323-328. <https://doi.org/10.1007/s12594-017-0720-x>
- Shah, S. B. A., & Shah, S. H. A. (2021). Hydrocarbon Generative Potential of Cretaceous and Jurassic Deposits in the Ahmedpur East Oilfield Subsurface, Punjab Platform, Pakistan. *Journal of the Geological Society of India*, 97(8), 923-926. <https://doi.org/10.1007/s12594-021-1792-1>
- Shah, S. B. A. (2022). Evaluation of organic matter in Sakesar and Patala formations in southern and northern Potwar Basin, Pakistan. *Petroleum Science and Technology*, 41(21), 2071-2087. <https://doi.org/10.1080/10916466.2022.2105360>
- Shah, S. B. A. (2023). Evaluation of mixed organic-rich carbonate and shale rocks of Meyal oilfield using an integrated palynofacies, geochemical and petrophysical approaches. *Petroleum Science and Technology*. <https://doi.org/10.1080/10916466.2023.2175864>
- Shah, S. B. A., Shah, S. H. A., & Jamshed, K. (2023). An integrated palynofacies, geochemical and petrophysical analysis for characterizing mixed organic-rich carbonate and shale rocks of Dhulian oilfield Potwar Basin, Pakistan: Insights for multiple source and reservoir rocks evaluation. *Geoenergy Science and Engineering*, 221, 111236. <https://doi.org/10.1016/j.petrol.2022.111236>
- Shah, S. M. I. (2009). *Stratigraphy of Pakistan*. Ministry of Petroleum and Natural Resources, Geological Survey of Pakistan, Memoirs of the Geological Survey of Pakistan, 22.
- Su, F., He, X., Dai, M., Yang, J., Hamanaka, A., Yu, Y., & Li, J. (2023). Estimation of the cavity volume in the gasification zone for underground coal gasification under different oxygen flow conditions. *Energy*, 285, 129309. <https://doi.org/10.1016/j.energy.2023.129309>
- Tissot, B. P., & Welte, D. H. (1984). *Petroleum Formation and Occurrence*, 2nd Edition. Springer-Verlag, Berlin, Heidelberg, 699 pp.
- Tucker, M. E. (2003). *Sedimentary Rocks in the Field*. John Wiley and Sons.
- Wang, Y., Peng, J., Wang, L., Xu, C., & Dai, B. (2023). Micro-macro evolution of mechanical behaviors of thermally damaged rock: A state-of-the-art review. *Journal of Rock Mechanics and Geotechnical Engineering*. <https://doi.org/10.1016/j.jrmge.2023.11.012>
- Welte, D. H. (1972). Petroleum exploration and organic geochemistry. *Journal of Geochemical Exploration*, 1(1), 117-136. [https://doi.org/10.1016/0375-6742\(72\)90009-X](https://doi.org/10.1016/0375-6742(72)90009-X)
- Waples, D. W. (1985). *Geochemistry in Petroleum Exploration*. Springer, Dordrecht. pp. 121-154.
- Wei, X., Bai, X., Wen, X., Liu, L., Xiong, J., & Yang, C. (2023). A large and overlooked Cd source in karst areas: The migration and origin of Cd during soil formation and erosion. *Science of The Total Environment*, 895, 165126. <https://doi.org/10.1016/j.scitotenv.2023.165126>
- Xi, Z., Xiaoming, Z., Jiawang, G., Shuxin, L., & Tingshan, Z. (2023). Karst topography paces the deposition of lower Permian, organic-rich, marine-continental transitional shales in the southeastern Ordos Basin, northwestern China. *AAPG Bulletin*. DOI:10.1306/11152322091
- Xiao, D., Liu, M., Li, L., Cai, X., Qin, S., Gao, R., & Li, G. (2023). Model for economic evaluation of closed-loop geothermal systems based on net present value. *Applied Thermal Engineering*, 231, 121008. <https://doi.org/10.1016/j.applthermaleng.2023.121008>
- Xu, Z., Li, X., Li, J., Xue, Y., Jiang, S., Liu, L., & Sun, Q. (2022a). Characteristics of Source Rocks and Genetic Origins of Natural Gas in Deep Formations, Gudian Depression, Songliao Basin, NE China. *ACS Earth and Space Chemistry*, 6(7), 1750-1771. <https://doi.org/10.1021/acsearthspacchem.2c00065>
- Xu, J., Zhou, G., Su, S., Cao, Q., & Tian, Z. (2022b). The Development of A Rigorous Model for Bathymetric Mapping from Multispectral Satellite-Images. *Remote Sensing*, 14(10). <https://doi.org/10.3390/rs14102495>
- Yan, T., Xu, R., Sun, S., Hou, Z., & Feng, J. (2024). A real-time intelligent lithology identification method based on a dynamic felling strategy weighted random forest algorithm. *Petroleum Science*, 21(2), 1135-1148. <https://doi.org/10.1016/j.petsci.2023.09.011>
- Yang, L., Yang, D., Zhang, M., Meng, S., Wang, S., Su, Y., ... Xu, L. (2024). Application of nano-scratch technology to identify continental shale mineral composition and distribution length of bedding interfacial transition zone - A case study of Cretaceous Qingshankou formation in Gulong Depression, Songliao Basin, NE China. *Geoenergy Science and Engineering*, 234, 212674. <https://doi.org/10.1016/j.geoen.2024.212674>
- Yang, L., Wang, H., Xu, H., Guo, D., & Li, M. (2023). Experimental study on characteristics of water imbibition and ion diffusion in shale reservoirs. *Geoenergy Science and Engineering*, 229, 212167. <https://doi.org/10.1016/j.geoen.2023.212167>
- Yasin, Q., Baklouti, S., Khalid, P., Ali, S. H., Boateng, C. D., & Du, Q. (2021). Evaluation of shale gas reservoirs in complex structural enclosures: A case study from Patala Formation in the Kohat-Potwar Plateau, Pakistan. *Journal of Petroleum Science and Engineering*, 198, 108225. <https://doi.org/10.1016/j.petrol.2020.108225>
- Yin, L., Wang, L., Li, T., Lu, S., Yin, Z., Liu, X., ... Zheng, W. (2023a). U-Net-STN: A Novel End-to-End Lake Boundary Prediction Model. *Land*, 12(8), 1602. <https://doi.org/10.3390/land12081602>
- Yin, L., Wang, L., Keim, B. D., Konsoer, K., Yin, Z., Liu, M., ... Zheng, W. (2023b). Spatial and wavelet analysis of precipitation and river discharge during operation of the Three Gorges Dam, China. *Ecological Indicators*, 154, 110837. <https://doi.org/10.1016/j.ecolind.2023.110837>

- Yin, H., Wu, Q., Yin, S., Dong, S., Dai, Z., ... Soltanian, M. R. (2023c). Predicting mine water inrush accidents based on water level anomalies of borehole groups using long short-term memory and isolation forest. *Journal of Hydrology*, 616, 128813. <https://doi.org/10.1016/j.jhydrol.2022.128813>
- Yin, L., Wang, L., Li, T., Lu, S., Tian, J., Yin, Z., & Zheng, W. (2023d). U-Net-LSTM: Time Series-Enhanced Lake Boundary Prediction Model. *Land*, 12(10), 1859. <https://doi.org/10.3390/land12101859>
- Yu, H., Wang, H., & Lian, Z. (2022). An Assessment of Seal Ability of Tubing Threaded Connections: A Hybrid Empirical-Numerical Method. *Journal of Energy Resources Technology*, 145(5). <https://doi.org/10.1115/1.4056332>
- Yu, J., Zhu, Y., Yao, W., Liu, X., Ren, C., Cai, Y., ... Tang, X. (2021). Stress relaxation behaviour of marble under cyclic weak disturbance and confining pressures. *Measurement*, 182, 109777. <https://doi.org/10.1016/j.measurement.2021.109777>
- Zahid, M., Khan, A., ur Rashid, M., Saboor, A., & Ahmad, S. (2014). Structural interpretation of Joya Mair oil field, south Potwar, Upper Indus Basin, Pakistan, using 2D seismic data and petrophysical analysis. *Journal of Himalayan Earth Sciences*, 47(1), 73-86.
- Zhang, S., Bai, X., Zhao, C., Tan, Q., Luo, G., Wang, J., & Xi, H. (2021). Global CO₂ Consumption by Silicate Rock Chemical Weathering: Its Past and Future. *Earth's Future*, 9(5), e1938E-e2020E. <https://doi.org/10.1029/2020EF001938>
- Zhou, G., Su, S., Xu, J., Tian, Z., & Cao, Q. (2023). Bathymetry Retrieval From Spaceborne Multispectral Subsurface Reflectance. *IEEE Journal of Selected Topics in Applied Earth Observations and Remote Sensing*, 16, 2547-2558. <https://doi.org/10.1109/JSTARS.2023.3249789>
- Zhou, G., Zhang, H., Xu, C., Zhou, X., Liu, Z., Zhao, D., ... Wu, G. (2023). A Real-Time Data Acquisition System for Single-Band Bathymetric LiDAR. *IEEE Transactions on Geoscience and Remote Sensing*, 61. <https://doi.org/10.1109/TGRS.2023.3282624>
- Zhu, G., Yong, L., Zhao, X., Liu, Y., Zhang, Z., Xu, Y., ... Wang, L. (2022). Evaporation, infiltration and storage of soil water in different vegetation zones in the Qilian Mountains: a stable isotope perspective. *Hydrology and Earth System Sciences*, 26(14), 3771-3784. <https://doi.org/10.5194/hess-26-3771-2022>